CONCEALED WEAPON DETECTION USING DIGITAL IMAGE PROCESSING

Abstract:

We have recently witnessed the series of bomb blasts in Mumbai. Bombs went of in buses and underground stations. And killed many and left many injured. On July 13th seven explosions took place with in one hour. And left the world in shell shock and the Indians in terror.

This situation is not limited to Mumbai but it can happen anywhere and any time in the world. People think bomb blasts can't be predicted before handled. Here we show you the technology, which predicts the suicide bombers and explosion of weapons through IMAGE PROCESSING FOR CONCLEAD WEAPON DETECTION.

The detection of weapons concealed underneath a person's clothing is very much important to the improvement of the security of the general public as well as the safety of public assets like airports, buildings, and railway stations etc. Manual screening procedures for detecting concealed weapons such as handguns, knives, and explosives are common in controlled access settings like airports, entrances to sensitive buildings and public events. It is desirable sometimes to be able to detect concealed weapons from a standoff distance, especially when it is impossible to arrange the flow of people through a controlled procedure

In the present paper we describe the concepts of the technology 'CONCEALEAD WEAPON DETECTION' the sensor improvements, how the imaging takes place and the challenges. And we also describe techniques for simultaneous noise suppression, object enhancement of video data and show some mathematical results.

Key Words: *Explosions, Concealed Weapons, Video Data.*

Conclusion: Imaging techniques based on a combination of sensor technologies and processing will potentially play a key role in addressing the concealed weapon detection problem. In this Paper, we first briefly reviewed the sensor technologies being investigated for the CWD application. Of the various methods being investigated, passive MMW imaging sensors Offer the best near-term potential for providing a noninvasive method of observing metallic and plastic objects concealed underneath common clothing. Recent advances in MMW sensor technology have led to video-rate (30 frames/s) MMW cameras. However, MMW cameras alone cannot provide useful information about the detail and location of the individual being monitored. To enhance the practical values of passive MMW cameras, sensor fusion approaches using MMW and IR, or MMW and EO cameras are being described. By integrating the complementary information from different sensors, a more effective CWD system is expected. In the second part of this paper, we provided a survey of the image processing techniques being developed to achieve this goal. Specifically, topics such as MMW image/video enhancement, filtering, registration, fusion, extraction, description, and recognition were discussed. A preliminary study on the performance of several shape descriptors that show promising results has also been reported in this paper.

Introduction:

Till now the detection of concealed weapons is done by manual screening procedures. To control the explosives in some places like airports, sensitive buildings, famous constructions etc. But these manual screening procedures are not giving satisfactory results, because this type of manual screenings procedures screens the person when the person is near the screening machine and also some times it gives wrong alarm indications so we are need of a technology that almost detects the weapon by scanning. This can be achieved by imaging for concealed weapons.

The goal is the eventual deployment of automatic detection and recognition of concealed weapons. It is a technological challenge that requires innovative solutions in sensor technologies and image processing.

The problem also presents challenges in the legal arena; a number of sensors based on different phenomenology as well as image processing support are being developed to observe objects underneath people's clothing.

Imaging Sensors:

These imaging sensors developed for CWD applications depending on their portability, proximity and whether they use active or passive illuminations. The different types of imaging sensors for CWD based are shown in following table.

1.Infrared Imager:

Infrared imagers utilize the temperature distribution information of the target to form an image. Normally they are used for a variety of night-vision applications, such as viewing vehicles and people. The underlying theory is that the infrared radiation emitted by the human body is absorbed by clothing and then re-emitted by it. As a result, infrared radiation can be used to show the image of a concealed weapon only when the clothing is tight, thin, and stationary. For normally loose clothing, the emitted infrared radiation will be spread over a larger clothing area, thus decreasing the ability to image a weapon.

2. P M W Imaging Sensors:

First Generation:

Passive millimeter wave (MMW) sensors measure the apparent temperature through the energy that is emitted or reflected by sources. The output of the sensors is a function of the emissive of the objects in the MMW spectrum as measured by the receiver. Clothing penetration for concealed weapon detection is made possible by MMW sensors due to the low emissive and high reflectivity of objects like metallic guns. In early 1995, the MMW data were obtained by means of scans using a single detector that

Took up to 90 minutes to generate one image.

Following figure1 (a) shows a visual image of a person wearing a heavy sweater that conceals two guns made with metal and ceramics. The corresponding 94-GHz radiometric image figure1 (b) was obtained by scanning a single detector across the object plane using a mechanical scanner. The radiometric image clearly shows both firearms.

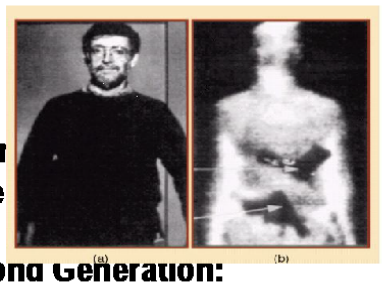

Figu MMW image of a person concealing 2 guns bene

Second Generation:

Recent advances in MMW sensor technology have led to video-rate (30 frames/s) MMW cameras .One such camera is the pupil-plane array from Terex Enterprises. It is
A 94-GHz radiometric pupil-plane imaging system that employs frequency scanning to achieve vertical resolution and uses an array of 32 individual wave-guide antennas for
Horizontal resolution. This system collects up to 30 frames/s of MMW data. Following figure shows the visible and second-generation MMW images of an individual
Hiding a gun underneath his jacket. It is clear from the figures 1(b), 2(b) that the image quality of the camera is degraded.

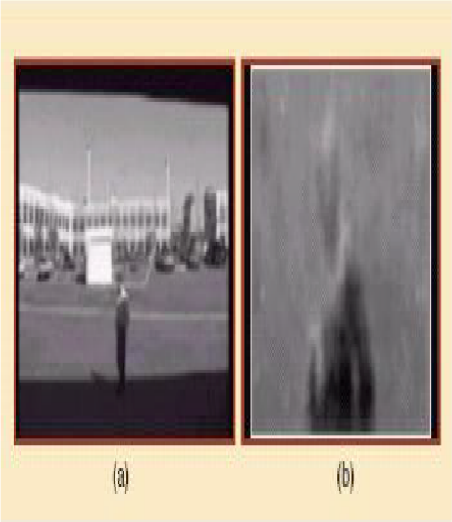

``

FIGURE 2a) visual image 2b) second-generation image of a person concealing a handgun beneath a jacket.

Cwd Through Image Fusion:

By fusing passive MMW image data and its corresponding infrared (IR) or electro-optical (EO) image, more complete information can be obtained; the information can then be utilized to facilitate concealed weapon detection. Fusion of an IR image revealing a concealed weapon and its corresponding MMW image has been shown to facilitate extraction of the concealed weapon. This is illustrated in the example given in following figure 3a) Shows an image taken from a regular CCD camera, and Figure3b) shows a corresponding MMW image. If either one of these two images alone is presented to a human operator, it is difficult to recognize the weapon concealed underneath the rightmost person's clothing. If a fused image as shown in Figure 3c) is presented, a human operator is able to respond with higher accuracy. This demonstrates the benefit of image fusion for the CWD application, which integrates complementary information
From multiple types of sensors.

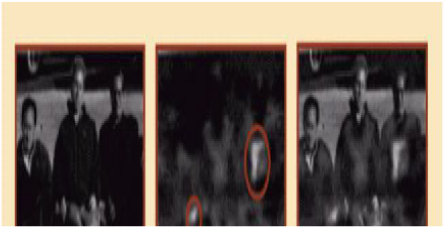

Imaging Processing Architecture:

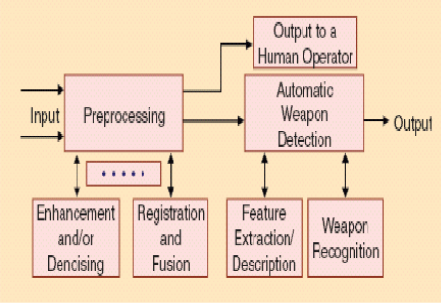

FIGURE 4: An Imaging Processing Architecture Overview For CWD

An image processing architecture for CWD is shown in Figure 4.The input can be multi sensor (i.e., MMW + IR, MMW + EO, or MMW + IR + EO) data or only the MMW data. In the latter case, the blocks showing registration and fusion can be removed from Figure 4. The output can take several forms. It can be as simple as a processed image/video sequence displayed on a screen; a cued display where potential concealed weapon types and locations are highlighted with associated confidence measures; a "yes," "no," or "maybe" indicator; or a combination of the above. The image processing procedures that have been investigated for CWD applications range from simple denoising to automatic pattern recognition.

Wavelet Approachs For Pre Processing:

Before an image or video sequence is presented to a human observer for operator-assisted weapon detection or fed into an automatic weapon detection algorithm, it is desirable to preprocess the images or video data to maximize their exploitation. The preprocessing steps considered in this section include enhancement and filtering for the removal of shadows, wrinkles, and other artifacts. When more than one sensor is used, preprocessing Must also include registration and fusion procedures.

1)Image Denoising & Enhancement Through Wavelets:

Many techniques have been developed to improve the quality of MMW images in this section, we describe a technique for simultaneous noise suppression and object enhancement of passive MMW video data and show some mathematical results.

Denoising of the video sequences can be achieved temporally or spatially. First, temporal denoising is achieved by motion compensated filtering, which estimates the motion trajectory of each pixel and then conducts a 1-D filtering along the trajectory.

This reduces the blurring effect that occurs when temporal filtering is performed without regard to object motion between frames. The motion trajectory of a pixel can be estimated by various algorithms such as optical flow methods, block-based methods, and
Bayesian methods. If the motion in an image sequence is not abrupt, we can restrict the search to a small region in the subsequent frames for the motion trajectory. For additional denoising and object enhancement, the technique employs a wavelet transform
Method that is based on multi scale edge representation.
The approach provides more flexibility and selectivity with less blurring. Furthermore, It offers a way to enhance objects in low-contrast images. Let ?1 *(x, y)* and *?2 (x, y)* be wavelets for *x* and *y* directions of an image, respectively. The ***dyadic wavelet transform*** of a function *f (x, y)* at *(x, y)* is defined as

$$W_{2^j}^k f(x,y) = f * \psi_{2^j}^k(x,y), k = 1,2 \qquad (1)$$

Where * represents the convolution operator, j is a wavelet decomposition level, and

$$\psi_{2^j}^k(x,y) = \frac{1}{2^j}\psi\left(\frac{x}{2^j}, \frac{y}{2^j}\right), k = 1,2. \qquad (2)$$

$$(W_{2^j}^1 f(x,y), W_{2^j}^2 f(x,y))$$

Then the vector contains the gradient information of f (x, y) at a point (x, y) the multiscaled edge representation G_{2J} (f) of an image at a level j is obtained by the magnitude P_{2J} f (x, y) and Θ_{2J} f (x, y) of the gradient vector

$$(W_{2^j}^1 f(x,y), W_{2^j}^2 f(x,y))$$

It is defined as

$$\begin{aligned} G_{2^j}(f) = \{&[(x_i, y_i), \nabla_{2^j} f(x_i, y_i)] | \rho_{2^j} f(x_i, y_i) \\ &\text{has local maximum at } (x_i, y_i) \\ &\text{along the direction } \theta_{2^j} f(x_i, y_i)\} \end{aligned} \qquad (3)$$

Where the magnitude and angle of the gradient are defined by

$$\rho_{2^j} f(x,y) \equiv \left\{\left[W_{2^j}^1 f(x,y)\right]^2 + \left[W_{2^j}^2 f(x,y)\right]^2\right\}^{1/2} \qquad (4)$$

$$\theta_{2^j} f(x,y) \equiv \arctan\left[\frac{W_{2^j}^2 f(x,y)}{W_{2^j}^1 f(x,y)}\right]. \qquad (5)$$

The multiscale edge representation *G2 j(f)* denotes a collection of local maxima of the magnitude *?2 j f(x, y)* at a point *(xi, yi)* along the direction *?2 j f(x, y)*. The wavelet transform based denoising

and enhancement technique is achieved by manipulating *G2 j(f)*. By suppressing the noisy edges below a predefined threshold in the finer scales, noise can be reduced while most of the true edges are preserved. To avoid removing

True edges accidentally in lower scales, where true edges generally become smaller, variable thresholds can be applied depending on scales. Enhancement of the image contrast is performed by stretching the multiscale edges in *G2 j(f)*. A denoised and

Enhanced image is reconstructed from the modified edges by the inverse wavelet transform; above Figure shows the results of this technique. In above figure 5(a), which shows a frame taken from the sample video sequence, the concealed gun does not show clearly

Because of noise and low contrast. The images in Figure 5(b) show the denoised frame by motion-compensated filtering. The frame was then spatially denoised and enhanced by the wavelet transform methods. Four decomposition levels were used and edges in

The fine scales were detected using the magnitude and angles of the gradient of the multiscale edge representation. The threshold for denoising was 15% of the maximum gradient at each scale. Figure 5(c) shows the final results of the contrast enhanced and

Demised frames. Note that the image of the handgun on the chest of the subject is more apparent in the enhanced frame than it is in the original frame. However, spurious features such as glint are also enhanced; higher-level procedures such as pattern

Recognition has to be used to discard these undesirable features.

Ii) Clutter Filtering:

Clutter filtering is used to remove unwanted details (shadows, wrinkles, imaging artifacts, etc.) that are not needed in the final image for human observation, and can adversely affect the performance of the automatic recognition stage. This helps improve the recognition performance, either operator-assisted or automatic. For this purpose, morphological filters have been employed. Examples of the use of morphological filtering for noise removal are provided through the complete CWD example given in Figure. A complete description of the example is given in a later section.

Iii) Registration Of Multi Sensor Images:

As indicated earlier, making use of multiple sensors may increase the efficacy of a CWD system. The first step toward image fusion is a precise alignment of images (i.e., image registration).

Very little has been reported on the registration problem for the CWD application. Here, we describe a registration approach for images taken at the same time from different but

Nearly collocated (adjacenand parallel) sensors based on the maximization of mutual information (MMI) criterion. MMI states that two images are registered when their mutual information (MI) reaches its maximum value. This can be expressed mathematically as the following:

$$\alpha^* = \arg\ opt(I(F(\tilde{x}), R(T_\alpha(\tilde{x})))) \quad (6)$$

Where *F* and *R* are the images to be registered. *F* is referred to as the *floating image*, whose pixel coordinates *(˜x)* are to be mapped to new coordinates on the *reference image R*. The reference image *R* is to be resampled according to the positions defined by

The new coordinates *Ta(˜x)*, where *T* denotes the transformation model, and the dependence of *T* on its associated parameters *a* is indicated by the use of notation *Ta*. *I* is the MI similarity measure calculated over the region of overlap of the two images and

Can be calculated through the joint histogram of the two images the above criterion says that the two images *F* and *R* are registered through *Ta** when *a** globally optimizes the MI measure, a two-stage registration algorithm was developed

For the registration of IR images and the corresponding MMW images of the first generation. At the first stage, two human silhouette extraction algorithms were developed, followed by a binary correlation to coarsely register the two images. The purpose was to provide an initial search point close to the final solution

For the second stage of the registration algorithm based on the MMI criterion. In this manner, any local optimizer can be employed to maximize the MI measure.

One registration result obtained by this approach is illustrated through the example

Given in Figure 6.

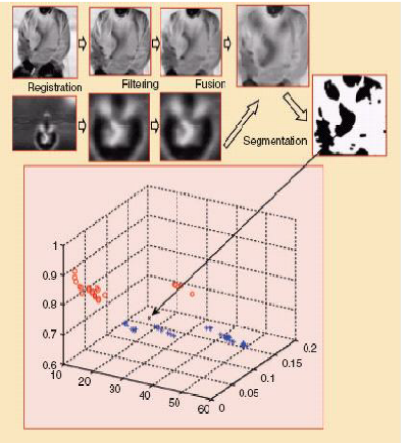

FIGURE 6: A CWD EXAMPLE

1v) Image Decomposition:

The most straightforward approach to image fusion is to take the average of the source images, but this can produce undesirable results such as a decrease in contrast. Many of the advanced image fusion methods involve multi resolution image decomposition based on the wavelet transform. First, an image pyramid is constructed for each source image by applying the wavelet transform to the source images. This transform domain representation emphasizes important details of the source images at different scales, which is useful for choosing the best fusion rules. Then, using a feature

Selection rule, a fused pyramid is formed for the composite image from the pyramid coefficients of the source images. The simplest feature selection rule is choosing the maximum of the two corresponding transform values. This allows the

Integration of details into one image from two or more images. Finally, the composite image is obtained by taking an inverse pyramid transform of the composite wavelet representation. The process can be applied to fusion of multiple source imagery. This

Type of method has been used to fuse IR and MMW images for CWD application [7]. The first fusion example for CWD application is given in Figure 7. Two IR images taken from separate IR cameras from different viewing angles are considered in this case. The advantage of image fusion for this case is clear since we can observe a complete gun shape only in the fused image. The second fusion example, fusion of IR and MMW images, is provided in Figure

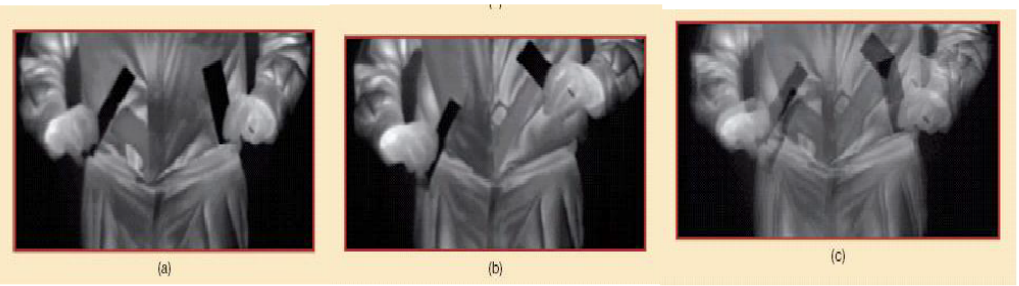

FIGURE 7: (a) and (b) are original I R images (c) is fused image

Automatic Weapon Detection:

After preprocessing, the images/video sequences can be displayed for operator-assisted weapon detection or fed into a weapon detection module for automated weapon detection. Toward this aim, several steps are required, including object extraction, shape description, and weapon recognition.

Segmentation For Object Extraction:

Object extraction is an important step towards automatic recognition of a weapon, regardless of whether or not the image fusion step is involved. It has been successfully used to extract the gun shape from the fused IR and MMW images. This could not be achieved using the original images alone. One segmented result from the fused IR and MMW image is shown in Figure 6. Another segmentation procedure applied successfully to MMW video sequences for CWD application is called the Slamani mapping Procedure (SMP). A block diagram of this procedure is given in Figure 8. The procedure

computes multiple important thresholds of the image data in the automatic threshold computation (ATC) stage for 1) regions with distinguishable intensity levels, and 2) regions with close intensity levels. Regions with distinguishable intensity levels have multi modal histograms, whereas regions with close intensity levels have overlapping histograms. The thresholds from both cases are fused to form the set of important thresholds in the scene. At the output of the ATC stage, the scene is quantized for each threshold value to obtain data above and below. Adaptive filtering is then used to perform homogeneous pixel grouping in order to obtain "objects" present at each threshold level. The resulting scene is referred to as a component image. Note that when the component images obtained for all thresholds are added together, they form a composite image that displays objects with different colors. Figure 9 shows the original scene and its corresponding composite image. Note that the weapon appears as a single object in the composite image.

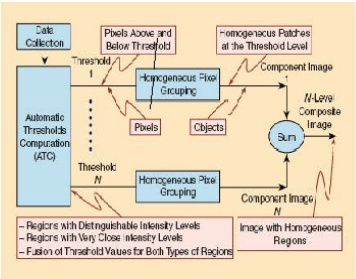

FIGURE 8: Block diagram of SMP

RESULTS OF SMP:

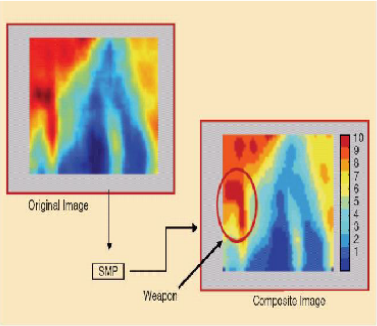

FIGURE 9: Original and composite images

1)Shape Description:

A) Moments:

It defines six shape descriptors based on the second- and third-order normalized moments that are translation, scale, and rotation invariant. The definitions of these six descriptors are provided below:

$$SD_1 = \eta_{20} + \eta_{02} \tag{7}$$

$$SD_2 = (\eta_{20} - \eta_{02})^2 + 4\eta_{11}^2 \tag{8}$$

$$SD_3 = (\eta_{30} - 3\eta_{12})^2 + (3\eta_{21} - \eta_{03})^2 \tag{9}$$

$$SD_4 = (\eta_{30} + \eta_{12})^2 + (\eta_{21} + \eta_{03})^2 \tag{10}$$

$$SD_5 = (\eta_{30} - 3\eta_{12})(\eta_{30} + \eta_{12})[(\eta_{30} + \eta_{12})^2 - 3(\eta_{21} + \eta_{03})^2] + (3\eta_{21} - \eta_{03})(\eta_{21} + \eta_{03}) \times [3(\eta_{30} + \eta_{12})^2 - (\eta_{21} + \eta_{03})^2] \tag{11}$$

$$SD_6 = (\eta_{20} - \eta_{02})\left[(\eta_{30} + \eta_{12})^2 - (\eta_{21} + \eta_{03})^2\right] + 4\eta_{11}(\eta_{30} + \eta_{12})(\eta_{21} + \eta_{03}) \tag{12}$$

``

Where *?p, q = (μp,q)/μ(p+q+2)/2* 0,0 is the normalized central moment with *μp,q = _(x- ¯x)p(y- ¯y)q* being the central

Moment. The performance of these six moment-based shape descriptors are examined in the next section. In addition to the moments of images, moments of region boundaries can be also defined. Let the coordinates of the *N* contour pixels of the object be described by an ordered set *(x(i), y(i))*, *i* = 1, 2, . . . , *N*. The Euclidean distance between the centroid, *(¯x, ¯y)* and the ordered sequence of the contour pixels of the shape is denoted as *d(i)*, *i* = 1, 2, . . . , *N*. This set forms a single-valued 1D unique representation

Of the contour. Based on the set *d(i)*, the *p*th moment is defined as

$$m_p = \frac{1}{N}\sum_{i=1}^{N}[d(i)]^p \qquad (13)$$

and the pth order central moment is defined as

$$M_p = \frac{1}{N}\sum_{i=1}^{N}[d(i) - m_1]^p. \qquad (14)$$

Using these moment definitions, a measure that can be used to describe feature shapes is defined by

$$F_2 = \frac{(M_4)^{1/4} - (M_2)^{1/2}}{m_1}. \qquad (15)$$

Note that the value is dimensionless as well as rotation, scale, and translation invariant.

b) CIRCULARITY:

A dimensionless measure of shape compactness or circularity, C, is defined as

C = P2/A (16)

Where *P* is the length of the region perimeter and *A* is the area of the region. Compactness provides a measure of contour complexity versus area enclosed. In addition, it measures how circular or elongated the object is. A shape with a rough contour including several incursions will have a high value of C, indicating low compactness. It is clear that this quantity is independent of rotation, scale, and translation

Mathematical Analysis:

To evaluate the performance of each individual shape descriptor, a test is designed based on the available MMW video sequence. First, a set of 30 frames was selected from a
Sequence of MMW data. Objects from each frame were extracted using the SMP described previously. There were 166 total objects extracted, among which 28 were weapons, by observing the original video sequence. To determine the performance of
Each shape descriptor, the probability of detection (PD) versus probability of
false alarm (PFA) is plotted by choosing different thresholds
for each of the shape descriptors.

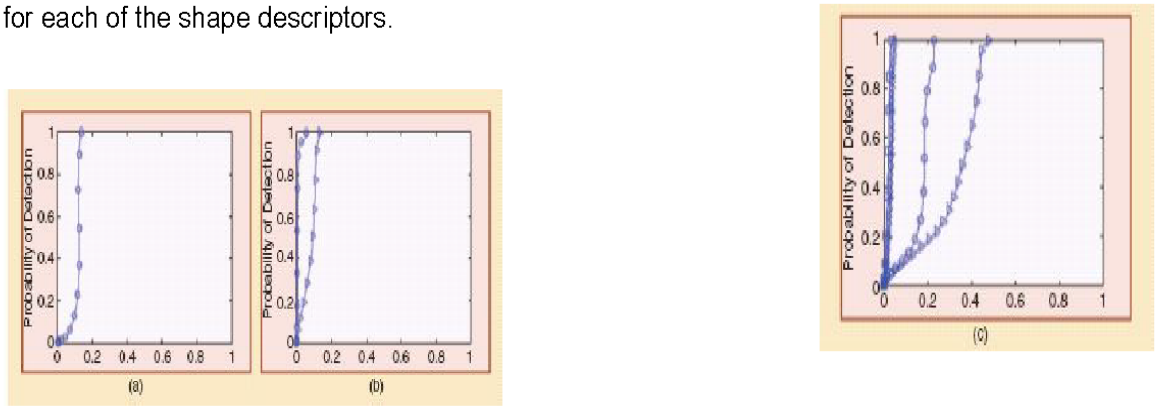

FIGURE 10(A) PD Versus PFA For C (0), (B) For SD (7) And SD (8), (C) SD (1) To SD (6)

Figure 10(a) shows that when all the weapons are detected (PD = 1.00), the PFA is about 0.13. Figure 10(b) shows the results obtained when the FD-based measures *SD*7 and *SD*8
Are used. It shows that the sum of the magnitude of the Fds results in better performance with less PFA than using the magnitude of the combination of the positive and corresponding negative phases of the FDs. Finally, Figure 10(c) shows the results of using moment-based shape measures to the set of objects. The plots of PD versus PFA show that *SD*1 and *SD*2, which are based on second-order moments, are the worst behaved ones; whereas *SD*3 through *SD*6, based on third order moments, are the best behaved ones and result in small values of PFA while generating very close results.

Challenges:

There are several challenges ahead. One critical issue is the challenge of performing detection at a distance with high probability of detection and low probability of false alarm. Yet another difficulty to be surmounted is forging portable multisensor instruments. Also, detection systems go hand in hand with subsequent response by the operator, and system development should take into account the overall context of deployment.